

## Original Article

**Cite this article:** Cai M, Xu Z, Clift PD, Khim B-K, Lim D, Yu Z, Kulhanek DK, and Li T (2020) Long-term history of sediment inputs to the eastern Arabian Sea and its implications for the evolution of the Indian summer monsoon since 3.7 Ma. *Geological Magazine* **157**: 908–919. <https://doi.org/10.1017/S0016756818000857>

Received: 27 March 2018  
Revised: 7 November 2018  
Accepted: 18 November 2018  
First published online: 27 December 2018




**Keywords:**

Arabian Sea; clay minerals; Deccan Traps; Indian summer monsoon; Indus River; International Ocean Discovery Program; IODP Site U1456

**Author for correspondence:**

Zhaokai Xu, Emails: [zhaokaixu@qdio.ac.cn](mailto:zhaokaixu@qdio.ac.cn) and Tiegang Li, Email: [tgli@fio.org.cn](mailto:tgli@fio.org.cn)

# Long-term history of sediment inputs to the eastern Arabian Sea and its implications for the evolution of the Indian summer monsoon since 3.7 Ma

Mingjiang Cai<sup>1,2,3</sup> , Zhaokai Xu<sup>1,2,\*</sup>, Peter D. Clift<sup>4,5</sup>, Boo-Keun Khim<sup>6</sup> , Dhongil Lim<sup>7</sup>, Zhaojie Yu<sup>1</sup>, Denise K. Kulhanek<sup>8</sup>  and Tiegang Li<sup>2,3,9,\*</sup>

<sup>1</sup>CAS Key Laboratory of Marine Geology and Environment, Institute of Oceanology, Chinese Academy of Sciences, Qingdao 266071, China; <sup>2</sup>Laboratory for Marine Geology, Qingdao National Laboratory for Marine Science and Technology, Qingdao 266061, China; <sup>3</sup>University of Chinese Academy of Sciences, Beijing 100049, China; <sup>4</sup>Department of Geology and Geophysics, Louisiana State University, Baton Rouge, LA 70803, USA; <sup>5</sup>Research Center for Earth System Science, Yunnan University, Kunming, Yunnan Province, 650091, China; <sup>6</sup>Department of Oceanography, Pusan National University, Busan 46241, Republic of Korea; <sup>7</sup>South Sea Research Institute, Korea Institute of Ocean Science & Technology, Geoje 53201, Republic of Korea; <sup>8</sup>International Ocean Discovery Program, Texas A&M University, College Station, TX 77845, USA and <sup>9</sup>Key Laboratory of Marine Sedimentology and Environmental Geology, First Institute of Oceanography, SOA, Qingdao 266061, China

**Abstract**

We present a new set of clay mineral and grain-size data for the siliciclastic sediment fraction from International Ocean Discovery Program (IODP) Site U1456 located in the eastern Arabian Sea to reconstruct the variabilities in the continental erosion and weathering intensity in the western Himalaya, elucidate the sediment source-to-sink processes and discuss the potential controls underlying these changes since 3.7 Ma. The clay minerals mainly consist of smectite (0–90%, average 44%) and illite (3–90%, average 44%), with chlorite (1–26%, average 7%) and kaolinite (0–19%, average 5%) as minor components. The compositional variations in the clay minerals at IODP Site U1456 suggest four phases of sediment provenance: the Indus River (phase 1, 3.7–3.2 Ma), the Indus River and Deccan Traps (phase 2, 3.2–2.6 Ma), the Indus River (phase 3, 2.6–1.2 Ma) and the Indus River and Deccan Traps (phase 4, 1.2–0 Ma). These provenance changes since 3.7 Ma can be correlated with variations in the Indian summer monsoon intensity. The siliciclastic sediments in the eastern Arabian Sea were mainly derived from the Indus River when the Indian summer monsoon was generally weak. In contrast, when the Indian summer monsoon intensified, the siliciclastic sediment supply from the Deccan Traps increased. In particular, this study shows that the smectite/(illite+chlorite) ratio is a sensitive tool for reconstructing the history of the variation in the Indian summer monsoon intensity over the continents surrounding the Arabian Sea since 3.7 Ma.

**1. Introduction**

The Asian summer monsoon intensity controls the surface weathering, erosion and sediment transport over the Asian continent, thereby influencing the transport of suspended particulate matter into the ocean by some of the largest rivers in the world (e.g. the Yangtze River, Yellow River, Mekong River, Red River, Pearl River, Indus River and Ganges River), as well as smaller regional rivers and the affecting sediment compositions in the depositional areas (e.g. Molnar *et al.* 1993; Curray, 1994; Clift *et al.* 2008; Tada *et al.* 2013 (and references therein), 2016; Liu *et al.* 2016). Evidences suggest that the tectonic evolution of the Himalayan region, particularly the weathering and erosion of the Himalayan Mountain Range, has been partially controlled by the intensity of Asian summer monsoon rainfall (Beaumont *et al.* 2001; Clift *et al.* 2008; Wan *et al.* 2012; Tada *et al.* 2013 (and references therein), 2016; Liu *et al.* 2016). The difficulty associated with the acquisition of long-term, continuous terrestrial core samples of weathering and erosion products from the Himalayan Mountain Range and the accurate determination of their chronologies makes it difficult to reconstruct the history of the variation of monsoon intensity over the geological record based on terrestrial sedimentary records. Conversely, due to the generally good continuity of marine sediment records, marine sediment analysis has been widely used to investigate the long-term history of climate change (Thiry, 2000; Phillips *et al.* 2014). By studying marine and terrestrial sediments in some regions controlled by the East Asian monsoon, previous researchers have found a close relationship between the East Asian monsoon intensity and the rates of weathering and erosion in the Himalayan region since the early Miocene (e.g. Liu *et al.* 2003; Wan *et al.* 2007, 2012; Clift *et al.* 2008, 2014; Sun *et al.* 2010; Tada *et al.* 2013 (and references therein), 2016; Liu *et al.* 2016). As a component of the

Asian monsoon system, the Indian monsoon (i.e. South Asian monsoon) intensity is also closely linked to the weathering and erosion rates of terrestrial sediment in the regions affected by the Indian monsoon and to the sedimentation rates in the corresponding areas of sediment accumulation. Consequently, a strong Indian monsoon often leads to intense weathering and erosion. Overall, monsoon rainfall is likely one of the primary factors controlling weathering and erosion in the Himalayan region (Derry & France-Lanord, 1996; Thiede *et al.* 2004; Clift *et al.* 2008; Kuwahara *et al.* 2010). Unfortunately, due to the difficulty associated with the acquisition of core samples, most existing studies on the Indian monsoon employed short piston and gravity cores limited to recent glacial–interglacial cycles (e.g. Overpeck *et al.* 1996; Fleitmann *et al.* 2003; Ivanova *et al.* 2003; Singh *et al.* 2006, 2011), and the few studies that delved into deeper time had a very low resolution (e.g. Clift *et al.* 2001, 2008; Pandey *et al.* 2016). Therefore, the relationship between the Indian monsoon evolution and the weathering and erosion of the Himalayan Mountain Range over long timescales is currently a topic of heavy debate. Some evidence suggests that the intensification of the Indian monsoon triggered the exhumation of the Greater Himalayas (Clift *et al.* 2008), whereas other research suggests that a shift in the intertropical convergence zone to above the Himalayan region was the primary driver of the rapid exhumation of the Greater Himalayas during the early Miocene (Armstrong & Allen, 2011; Allen & Armstrong, 2012).

The rapid uplift of the Tibetan Plateau and the Himalaya–Karakoram mountain system caused by the collisional compression between the Indian and Eurasian plates during the mid- and late Miocene and the intensification of the Indian monsoon is proposed to have caused intense weathering and erosion throughout the Himalayan region (Clift *et al.* 2001). In particular, some evidence suggests that the uplift that occurred during the middle Pliocene to early Pleistocene from 4 to 2 Ma may also have been responsible for the origins of the Asian monsoons and even of Northern Hemisphere glaciation (Rea, 1992). Specifically, large amounts of weathering and erosion products have been delivered into the Arabian Sea by rivers, including the Indus River, forming an extremely thick sedimentary deposit known as the Indus Fan (Clift *et al.* 2001; Garzanti *et al.* 2005). The intense weathering and erosion of the plateau have led to the absorption of large amounts of carbon dioxide (CO<sub>2</sub>) from the atmosphere, resulting in a significant decrease in global atmospheric CO<sub>2</sub> concentration, which in turn has resulted in global climate cooling (Raymo *et al.* 1988; Prell & Kutzbach, 1992; Molnar *et al.* 1993; France-Lanord & Derry, 1997; Rea *et al.* 1998; Sun *et al.* 1998; An *et al.* 2001; Wan *et al.* 2012). Therefore, reconstructing the long-term history of weathering and erosion in the Himalayan region and the delivery of the resultant products into the ocean by examining variations in the sedimentary composition of the Indus Fan is of great scientific significance to understanding tectonic activity, monsoon intensity and source-to-sink sediment transport.

Clay minerals have been widely used as a proxy to trace the sources of marine sediments, characterize the weathering intensity of sediments deposited in the ocean, and reconstruct the palaeoclimatic conditions of the potential source areas (Chamley, 1989; Liu *et al.* 2003; Alizai *et al.* 2012; Phillips *et al.* 2014; Xu *et al.* 2015; Yu *et al.* 2016). Variations in the clay mineral composition are closely related to the weathering intensities of the potential provenances of sediments. Changes in these chemical weathering intensities induced by palaeoclimatic and palaeoenvironmental variations in the source regions of sediments are ultimately detailed in the sedimentary record, as evidenced by studies from numerous

regions in Asia (e.g. Bouquillon *et al.* 1989; Sirocko & Lange, 1991; Prins *et al.* 2000; Thamban *et al.* 2002; Boulay *et al.* 2005; Liu *et al.* 2009; Colin *et al.* 2010; Xu *et al.* 2016; Wan *et al.* 2017). In this work, high-resolution clay mineral assemblage data from terrigenous sediments in the eastern Arabian Sea were collected, and their variations since 3.7 Ma were analysed. On this basis, we traced the sources of the clay fractions in detrital sediments and analysed the coupled relationship between the changes in the characteristics of the clay mineral assemblage and the Indian monsoon intensity across long-timescales.

## 2. Materials and methods

International Ocean Discovery Program (IODP) Site U1456 (16° 37.28' N, 68° 50.33' E) was cored in the eastern Arabian Sea in April–May 2015 (Fig. 1). Located within the Laxmi Basin between the western Indian shelf and the Laxmi Ridge, IODP Site U1456 is situated ~475 km from the west coast of India and ~820 km from the modern Indus River mouth. The site was cored to a total composite depth of 1109.4 m below the seafloor over five holes (U1456A–U1456E) at a water depth of 3640 m.

In this study, the upper ~500 m of the core composite depth below the seafloor (CCSF) from IODP Site U1456 was selected for analysis. A total of 309 sediment samples (U1456A, C, and D) were collected from this segment at intervals of 50–200 cm. No noticeable volcanic ash beds were observed in this segment (Fig. 2). From 0 to 120 m, the lithology of the studied sections consists primarily of carbonate ooze and clay interbeds. Between 120 and 360 m, the lithology of the studied sections consists of nannofossil-rich ooze interbedded with dark-grey sand and silt with a small number of thin mud layers. In addition, this interval contains many sand and silt layers. From 360 to 440 m, the lithology of the recovered sections is mainly nannofossil-rich clay. The core for the interval between 440 and 500 m contains a small number of thin clay and thick sand layers (Fig. 2).

The chronostratigraphic framework for the top ~500 m of the site was established based on 16 palaeomagnetic and micropalaeontological data points identified by the shipboard scientists during the expedition (Table 1). According to the age model (Fig. 2), the upper 500 m of the CCSF from IODP Site U1456 provides a generally continuous record of the last 3.7 Ma. It is worth noting that a ~0.45 Ma depositional hiatus spans between 2.39 and 1.93 Ma (Pandey *et al.* 2016). The sample ages were determined using linear interpolation and extension while assuming that the sedimentation rate remained unchanged between two adjacent age control points (Fig. 2).

The clay mineral composition was analysed using the X-ray diffraction (XRD) method on the oriented <2 µm siliciclastic fraction. To obtain the siliciclastic components of the sediment, the sample was pretreated with a sequential leaching procedure (Bayon *et al.* 2002; Gutjahr *et al.* 2007). First, an excess amount of 10 % acetic acid was used to remove carbonates from the sample in a 60 °C water bath for 2 h. Upon completion of the reaction, the sample was washed twice with deionized (DI) water and centrifuged. Then a 0.25 mol L<sup>-1</sup> hydroxylamine hydrochloride solution (in a 25% acetic acid medium) was used to remove ferromanganese oxides from the sample in an 85 °C water bath for 4 h. Upon completion of the reaction, the sample was washed twice with DI water and centrifuged. Afterward, a nitric acid (HNO<sub>3</sub>) – hydrogen peroxide (H<sub>2</sub>O<sub>2</sub>) mixture (prepared with 15 mL of 0.02 mol L<sup>-1</sup> HNO<sub>3</sub> and 25 mL of H<sub>2</sub>O<sub>2</sub>) was used to remove organic matter from the sample in a 60 °C water bath for 3 h. Upon completion of the

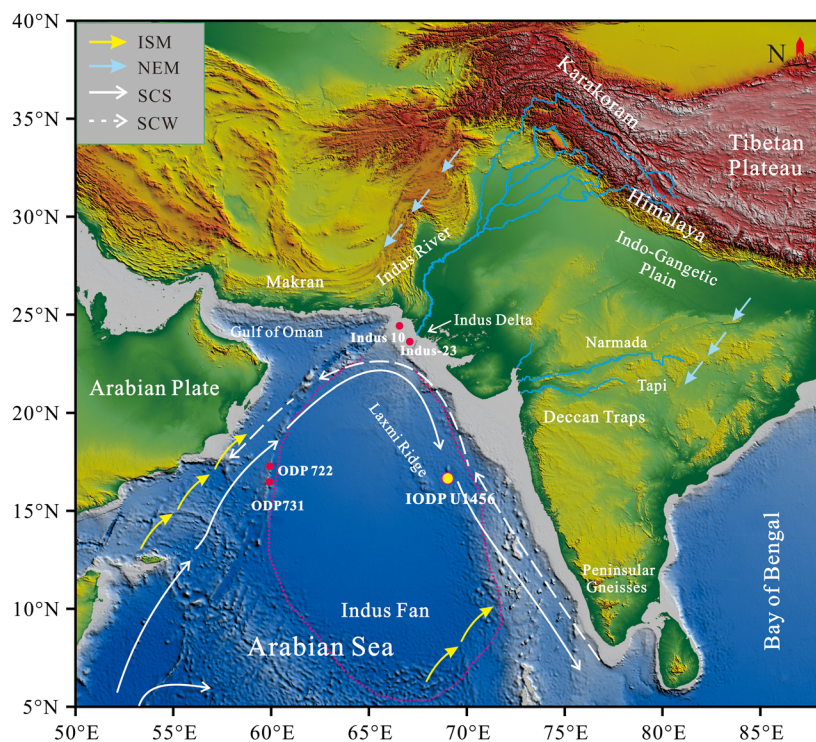


**Fig. 1.** Bathymetric map showing the location of IODP Site U1456 as well as the surrounding geological structures (i.e. the Tibetan Plateau, Arabian plate, Makran, Indo-Gangetic Plain, Deccan Traps and Peninsular Gneisses). Yellow circles: IODP Expedition 355 Site U1456; blue lines: major rivers and tributaries; pink circles: partly marine sediment cores mentioned in this paper (cores ODP Site 722, ODP Site 731, Indus10 and Indus-23); pink line: approximate extent of the fan after Kolla & Coumes (1987); ISM: Indian summer monsoon; NEW: northeast (winter) monsoon; SCS: the surface circulations in the Arabian Sea in the summer; SCW: the surface circulations in the Arabian Sea in the winter.

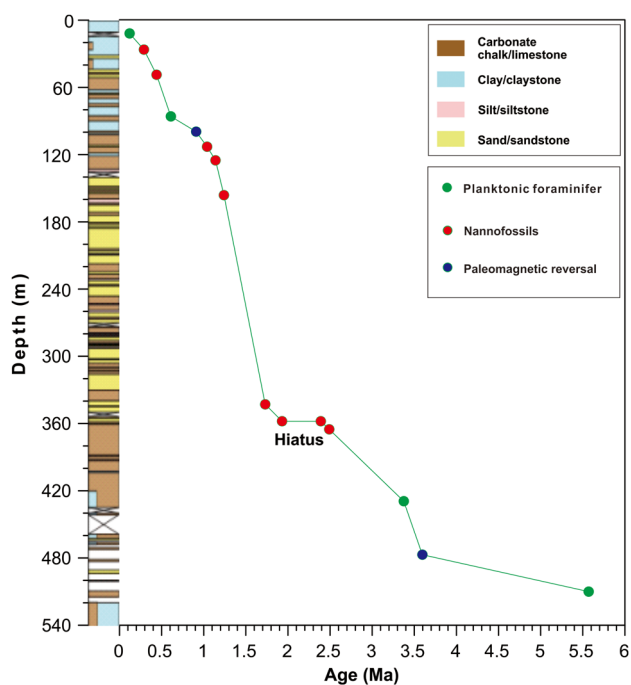


**Fig. 2.** Plot of age vs depth based on biostratigraphic and palaeomagnetostratigraphic data from IODP Site U1456 (Pandey *et al.* 2016).

reaction, the sample was washed twice with DI water and centrifuged. Finally, a 2 mol L<sup>-1</sup> anhydrous sodium carbonate solution was used to remove biogenic silica from the sample in an 85 °C water bath for 5 h. Upon completion of the reaction, the sample was washed twice with DI water and centrifuged. Afterward, the <2 μm fraction of the sample was extracted by centrifugation based on Stokes's principle, and oriented thin sections of clay minerals

were prepared. XRD measurements were performed on oriented thin sections that had been successively air-dried, saturated with ethylene glycol at 60 °C for 12 h and heated at 490 °C for 2 h to determine the clay mineral composition. The XRD analysis was performed on a D8 ADVANCE diffractometer at the Key Laboratory of Marine Geology and Environment, Chinese Academy of Sciences. The XRD peak areas of the four main clay minerals, namely, smectite, illite, chlorite and kaolinite, were obtained from the ethylene glycol saturation curve using the Topas 2P software. Based on the results, the relative percentage content of each clay mineral was calculated using the method proposed by Biscaye (1965). Semiquantitative estimates of the peak areas of the basal reflections for the main clay mineral groups (smectite: 17 Å; illite: 10 Å; and kaolinite/chlorite: 7 Å) were carried out on the glycolated samples. Replicate analysis of the same sample produced results with a relative error margin of ±5%. Smaller values of the full width at half maximum (FWHM) correspond to a higher mineral crystallinity. Additionally, the sediment detrital fraction was analysed to determine the grain size and mass accumulation rate (MAR). For the grain-size analysis, the sampling depth was the same as for the clay mineral analysis. Samples were measured after the removal of carbonates, organic matter and biogenic silica by acetic acid (10%), a nitric acid – hydrogen peroxide mixture (prepared with 15 mL of 0.02 mol L<sup>-1</sup> nitric acid and 25 mL of 30% hydrogen peroxide) and sodium carbonate (2 mol L<sup>-1</sup>), respectively. Grain-size measurements were carried out on a CILUS 1190 L apparatus at the Key Laboratory of Marine Geology and Environment, Chinese Academy of Sciences (measuring range: 0.5–2000 μm; relative repeatability error: <2%).

### 3. Results

#### 3.a. Clay mineralogy

The results (Fig. 3) show that the clay mineral assemblage of the sediments that have accumulated at IODP Site U1456 since

**Table 1.** Biostratigraphic and palaeomagnetostratigraphic ages of IODP Site U1456 (Pandey *et al.* 2016)

Event	Age (Ma)	Depth (m)
Top <i>Globigerinoides ruber</i> pink	0.12	11.87
Base <i>Emiliania huxleyi</i>	0.29	26.29
Top <i>Pseudoemiliania lacunosa</i>	0.44	48.72
Top <i>Globorotalia tosaensis</i>	0.61	85.91
C1n (o)	0.781	93.16
Top <i>Reticulofenestra asanoi</i>	0.91	99.51
Base reentrance <i>Gephyrocapsa</i> >4 $\mu\text{m}$	1.04	112.95
Base <i>Reticulofenestra asanoi</i>	1.14	125.11
Top <i>Gephyrocapsa</i> spp. >5.5 $\mu\text{m}$	1.24	156.19
Base <i>Gephyrocapsa</i> spp. >4 $\mu\text{m}$	1.73	342.87
Top <i>Discoaster brouweri</i>	1.93	357.94
Top <i>Discoaster pentaradiatus</i>	2.39	357.94
Top <i>Discoaster surculus</i>	2.49	365.16
Top <i>Sphaeroidinellopsis seminulina</i>	3.375	429.31
C2An.3n (o)	3.596	477.04
Base <i>Globorotalia tumida</i>	5.57	510

3.7 Ma consists primarily of smectite (average 44%) and illite (average 44%) and includes small amounts of kaolinite (average 5%) and chlorite (average 7%).

Markedly opposite variation trends are observed for the relative percentage contents of smectite and illite as well as smectite and chlorite since 3.7 Ma, as evidenced by the significant negative correlation coefficients between the smectite and illite contents ( $R = -0.98$ ) and between the smectite and chlorite contents ( $R = -0.77$ ). In contrast, a significant positive correlation is apparent between the illite and chlorite contents ( $R = 0.66$ ) (Fig. 4). Based on the profiles of the relative percentage contents of the four dominant clay mineral components (i.e. smectite, illite, chlorite and kaolinite), the clay mineral compositional variation is divided into four phases: phase 1 (from the early Pliocene to the mid-Pliocene (3.7–3.2 Ma)), phase 2 (the mid-Pliocene (3.2–2.6 Ma)), phase 3 (from the late Pliocene to the early Pleistocene (2.6–1.2 Ma)) and phase 4 (from the early Pleistocene to the present (1.2–0 Ma)) (Fig. 3).

In phase 1, illite is present in a relatively higher percentage (average 60%), followed by smectite (average 23%), with low contents of chlorite (average 10%) and kaolinite (average 7%). In phase 2, the smectite content (average 56%) is the highest, followed by illite (average 34%), chlorite (average 5%) and kaolinite (average 5%). In phase 3, illite (average 63%) is once again the primary clay fraction component, and smectite (average 22%) is the second most abundant component. Compared with phase 2, the chlorite content increases somewhat (average 11%), whereas the kaolinite content (average 4%) remains very low. In phase 4, smectite (average 59%) and illite (average 32%) are the primary and secondary components, respectively, whereas the chlorite (average 5%) and kaolinite (average 4%) contents are low (Fig. 3).

Since 3.7 Ma, the smectite crystallinity values in the terrigenous sediments have been relatively high, with an average value of  $1.35^\circ \Delta 2\theta$ . The trend in the variation in the smectite crystallinity is similar to that in the relative percentage content of smectite in the clay

fraction. The smectite contents are relatively low in phases 1 and 3, during which smectite has a relatively good crystallinity value (average  $1.20^\circ \Delta 2\theta$ ). In contrast, the higher smectite contents in phases 2 and 4 correspond to lower crystallinity values (average  $1.50^\circ \Delta 2\theta$ ). The average illite crystallinity value in phase 1 is  $0.45^\circ \Delta 2\theta$ , which increases to  $0.48^\circ \Delta 2\theta$  in phase 2 and subsequently decreases significantly in phases 3 (to  $0.40^\circ \Delta 2\theta$ ) and 4 (to  $0.37^\circ \Delta 2\theta$ ) (Fig. 3).

### 3.b. Mass accumulation rate (MAR)

Since 3.7 Ma, the MAR of the terrigenous sediment at IODP Site U1456 has undergone significant changes. During 3.7–3.4 Ma, the MAR was relatively high, with an average of  $33.6 \text{ g cm}^{-2} \text{ ka}^{-1}$ . Later, during 3.4–1.7 Ma, the MAR decreased significantly to an average of only  $11.9 \text{ g cm}^{-2} \text{ ka}^{-1}$ . During 1.7–1.2 Ma, the MAR increased to high levels and reached a maximum; during this period, the MAR had an average of  $89.9 \text{ g cm}^{-2} \text{ ka}^{-1}$ . During 1.2–0 Ma, although it fluctuated slightly, the MAR of the terrigenous sediments was relatively low, with an average of  $10.5 \text{ g cm}^{-2} \text{ ka}^{-1}$  (Fig. 3).

### 3.c. Grain size

The downcore variations in the median grain size (Md) and mean grain size (Mz) of the terrigenous sediments at IODP Site U1456 are shown in Figure 3. Similarly, based on the clear changes in both Md and Mz, the grain-size section can be divided into the same phases as the MAR of terrigenous sediments since 3.7 Ma. During 3.7–3.4 Ma, the Md and Mz fluctuated slightly, with average values of  $9.5 \mu\text{m}$  and  $9.5 \mu\text{m}$ , respectively. Later, during 3.4–1.7 Ma, Md and Mz both decreased significantly and showed a relatively stable trend, with average values of  $8.8 \mu\text{m}$  and  $8.6 \mu\text{m}$ , respectively. During 1.7–1.2 Ma, Md and Mz increased significantly and reached their maxima, with average values of  $17.8 \mu\text{m}$  and  $18.7 \mu\text{m}$ , respectively. During 1.2–0 Ma, despite some slight fluctuations, the Md and Mz values of the terrigenous sediments were relatively low, with average values of  $10.8 \mu\text{m}$  and  $10.1 \mu\text{m}$ , respectively (Fig. 3).

## 4. Discussion

### 4.a. Potential sources of the primary clay minerals

The mineralogical characteristics of clay are primarily controlled by the sediment source and the climate of the provenance region (Chamley, 1989; Wan *et al.* 2007; Alizai *et al.* 2012; Clift *et al.* 2014). Smectite primarily forms through the chemical weathering of igneous rocks (Chamley, 1989; Liu *et al.* 2003), while kaolinite forms in the warm, humid tropics and adjacent regions where intense leaching occurs (Chamley, 1989; Thamban *et al.* 2002). Illite and chlorite form through the breakdown of muscovite and biotite or from the erosion of sedimentary rocks and minerals, primarily in regions with dry, cold climates or in high-altitude regions where chemical weathering is very weak (Campbell & Claridge, 1982; Boulay *et al.* 2003). Accordingly, knowledge of the potential source areas of clay minerals constitutes a prerequisite for the interpretation of mineralogical and geochemical trends in marine sediments and the associated palaeoclimatic/palaeoenvironmental information (e.g. Liu *et al.* 2003; Hu *et al.* 2012; Clift *et al.* 2014; Wan *et al.* 2017). Previous research has shown that the clay minerals in the eastern Arabian Sea primarily originated from fluvial inputs, whereas aeolian dust inputs were negligible (Thamban *et al.* 2002; Avinash *et al.* 2016). Specifically, the clay minerals in the study area primarily originated from the Indus River, the Deccan Traps (the Tapti and the Narmada rivers),

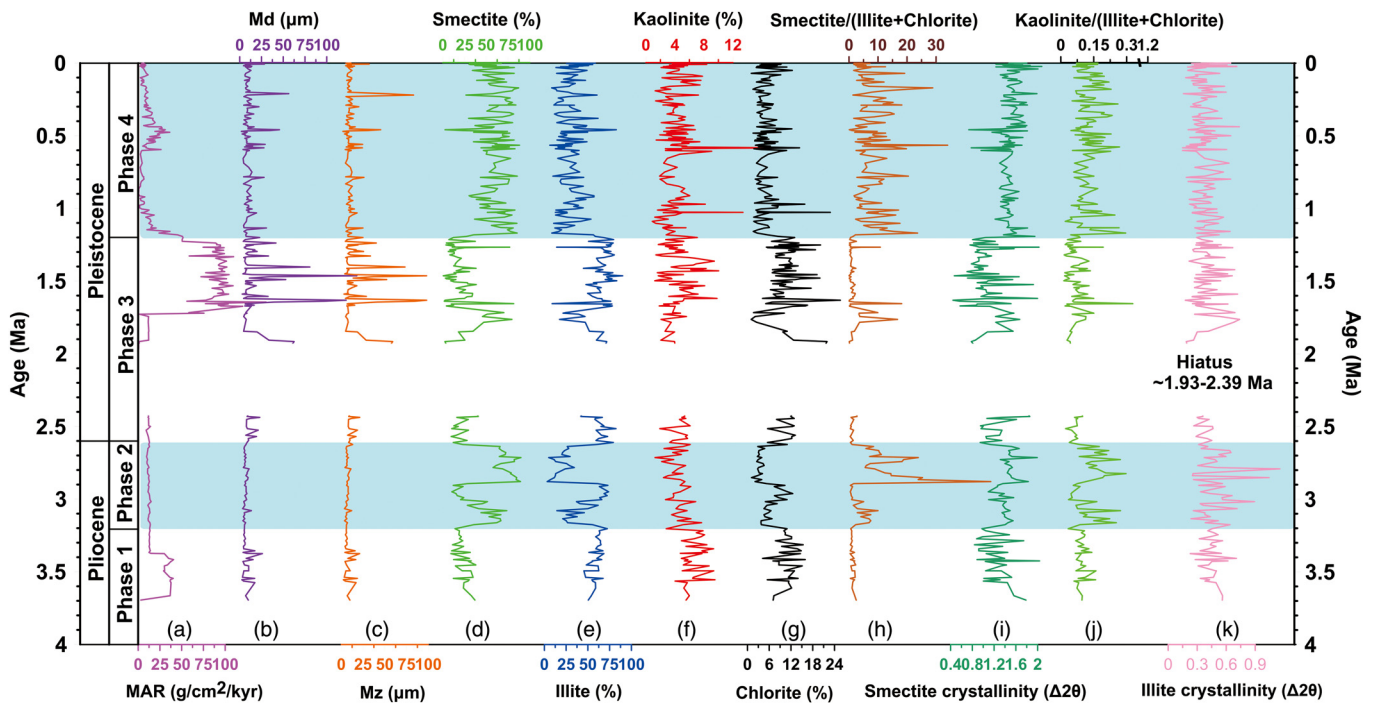


**Fig. 3.** Variations in the mass accumulation rate (MAR), median grain size (Md), and mean grain size (Mz) of terrigenous materials, as well as the clay mineral assemblages, ratios and crystallinities at IODP Site U1456.

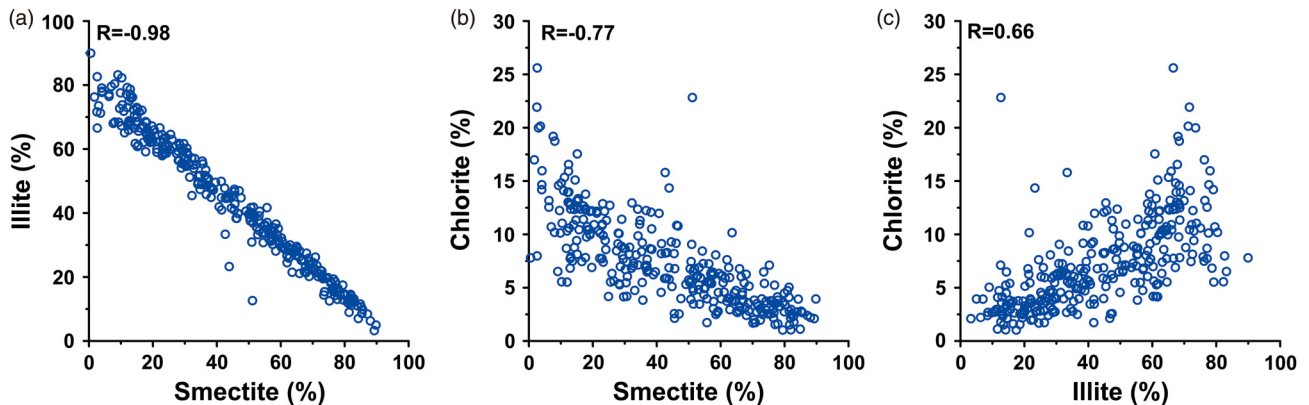


**Fig. 4.** Correlation analysis of smectite (%), illite (%) and chlorite (%) from IODP Site U1456.

and the gneiss region in the southern Indian subcontinent (Rao & Rao, 1995; Kessarkar *et al.* 2003). Furthermore, the primary clay minerals in the Indus River are illite, smectite and chlorite (Rao & Rao, 1995; Kessarkar *et al.* 2003; Alizai *et al.* 2012). As the primary source of the terrigenous sediments in the Arabian Sea (Prins *et al.* 2000), the Indus River delivers annually 250–675 Mt of suspended sediment into the Arabian Sea (Giosan *et al.* 2006; Milliman & Farnsworth, 2013). These detrital materials, upon reaching the ocean from the Indus River, can be transported by surface currents over distances of 1000–1500 km (Rao & Rao, 1995). Sediments derived from the Deccan Traps are primarily transported to the eastern Arabian Sea via rivers such as the Tapti River and the Narmada River (Kolla *et al.* 1981; Prins *et al.* 2000). Moreover, the Deccan Traps are covered by an extremely thick layer of basalt, which chemical weathering products therein are characterized by high contents of smectite, has

lasted for at least 9 Ma (Debrabant *et al.* 1991; Rao & Rao, 1995; Kessarkar *et al.* 2003; Phillips *et al.* 2014). In addition, the Deccan Traps contribute ~100 Mt of detrital material (Milliman & Farnsworth, 2013) to the eastern Arabian Sea annually, so this region represents another potential key sediment source. Elsewhere, the Precambrian gneiss, schist and charnockite in the gneiss region of southern India have formed kaolinite-rich clays due to intense chemical weathering under warm and humid conditions (Rao & Rao, 1995; Kessarkar *et al.* 2003); hence, the gneiss rocks from this region also constitute a potential source for the sediments in the eastern Arabian Sea. However, previous studies have shown that these clay minerals may have primarily settled along the western continental margin of India with relatively low river runoff (Rao & Rao, 1995; Kessarkar *et al.* 2003).

Based on the aforementioned preliminary investigation of potential source areas for the terrigenous sediments at IODP

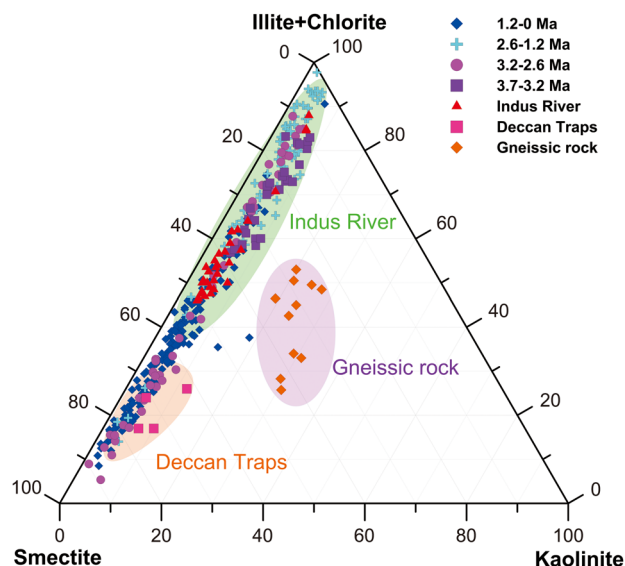


**Fig. 5.** Smectite–kaolinite–illite+chlorite ternary diagram showing the extents of the clay mineral compositions from IODP Site U1456. Published data of possible source materials, namely, those from the Indus River (Rao & Rao, 1995; Kessarkar *et al.* 2003; Alizai *et al.* 2012), the Deccan Traps (Rao & Rao, 1995; Kessarkar *et al.* 2003) and gneissic rocks (Rao & Rao, 1995; Kessarkar *et al.* 2003), are also plotted for comparison.

Site U1456, the provenances of the clay minerals in the eastern Arabian Sea are traced by comparing the clay minerals examined in this work with the clay mineral compositions of sediments from the potential source areas in the following section. Because the variation trends of the illite and chlorite contents at IODP Site U1456 are positively correlated ( $R = 0.66$ ), the illite and chlorite in the eastern Arabian Sea are considered to have originated from the same source. Thus, the sources of the sediments at IODP Site U1456 can be identified by plotting the clay mineral compositions on a smectite–kaolinite–illite+chlorite ternary diagram (Fig. 5).

The smectite–kaolinite–illite+chlorite ternary diagram for IODP Site U1456 for sediments from the Pliocene to Recent (Fig. 5) shows that the clay minerals at this site are compositionally similar to the clay minerals from the Indus River and the Deccan Traps; furthermore, a majority of the clay mineral compositions from this site are relatively similar to those from the Indus River (Rao & Rao, 1995; Kessarkar *et al.* 2003; Alizai *et al.* 2012). Therefore, IODP Site U1456 has primarily received clay mineral inputs from the Indus River since 3.7 Ma but has also received inputs from the Deccan Traps during certain phases. The clay mineral compositions during phases 1 and 3 are similar to the clay mineral compositions of the Indus River, indicating that the detrital clay minerals in the study area were primarily derived from the Indus River during these two phases (Rao & Rao, 1995; Kessarkar *et al.* 2003; Alizai *et al.* 2012). A relatively broad variability is evident in the clay mineral compositions at IODP Site U1456 during phases 2 and 4. In addition, the relative percentage content of smectite during these two phases is significantly higher than that of the clay originating from the Indus River and noticeably shifts toward that of the Deccan Traps source field. Thus, although the bulk of the clay minerals originated from the Indus River during phases 2 and 4, noticeable amounts were also derived from the Deccan Traps (Rao & Rao, 1995; Kessarkar *et al.* 2003). In contrast, the clay mineral composition in the gneiss region of southern India

differs significantly from the sample compositions examined in this work, indicating that the contribution of detrital clay minerals from the gneiss region to the study area is negligible (Fig. 5).

Smectite is generally formed through the chemical weathering of volcanic rocks (Chamley, 1989; Liu *et al.* 2004), and its crystallinity is closely related to the properties of the parent rock. Under normal circumstances, the crystallinity of smectite formed through the alteration of a basaltic parent rock is very low (Jeong *et al.* 2004). The smectite crystallinity values at IODP Site U1456 during phases 2 and 4 are lower than those during phases 1 and 3 (Fig. 3). This finding further supports the hypothesis that the Deccan Traps contributed greater amounts of low-crystallinity smectite formed through the alteration of basalt to the sedimentary clay fraction in the study area during phases 2 and 4.

#### 4.b. Palaeoenvironmental implications of the sediment provenance changes

The derivation of palaeoclimatic interpretations from mineralogical analyses requires the determination of potential sources in addition to an understanding of the mode and intensity of source-to-sink sediment transport (Gingele *et al.* 1998; Liu *et al.* 2003; Hu *et al.* 2012; Clift *et al.* 2014; Wan *et al.* 2017). On a tectonic timescale, marine sedimentation may be subject to the combined action of multiple factors, such as tectonic activity, terrigenous material supply changes, sea-level fluctuations and palaeomonsoon evolution (e.g. Clift & Blusztajn, 2005; Clift *et al.* 2008; Wan *et al.* 2012, 2017; Xu *et al.* 2015). Previous researchers studied the relationship between the characteristics of the clay mineral assemblage in the South China Sea and the East Asian monsoon intensity and found that the fluvial transport time of terrigenous sediment to the sea and the possible residence time are negligible on a tectonic timescale (Wan *et al.* 2007). Based on a comprehensive analysis of the MAR, particle size, and clay mineral composition characteristics, in addition to a review of previous research regarding the sources of the terrigenous sediments at IODP Site U1456, we select some reliable indicators to examine the variations in the sources and sedimentary processes of detrital clay found in sediments in the eastern Arabian Sea. Throughout the Arabian Sea, the intensification of the monsoon can enhance marine biological productivity; thus, the marine productivity in the study area is primarily controlled by the monsoon (Cabarcos *et al.* 2014; Gupta *et al.* 2015; Tripathi *et al.* 2017). Various biological productivity indicators, such as the total organic carbon (TOC) content and the stable isotope ratio of nitrogen ( $\delta^{15}\text{N}$ ), have been satisfactorily used to reconstruct the evolutionary history of the palaeomonsoon in the northern Indian Ocean (e.g. Overpeck *et al.* 1996; Sun *et al.* 2006; Huang *et al.* 2007; Gupta *et al.* 2015). In particular, based on TOC and  $\delta^{15}\text{N}$  data from sediments acquired from the same IODP site investigated in this study, previous studies have successfully reconstructed the evolutionary history of the Indian summer monsoon over the landmasses surrounding the eastern Arabian Sea since the late Miocene (Tripathi *et al.* 2017). Furthermore, the study by Tripathi *et al.* (2017) is significant for understanding the core scientific problem of the source-to-sink sediment transport process and its coupled relationship with the Indian summer monsoon intensity.

Clay mineral ratios can be successfully used to satisfactorily investigate the history of the variation in the palaeoclimate in a source area. For example, the smectite/(illite+chlorite) ratio represents the clay mineral proportions in the source area formed from

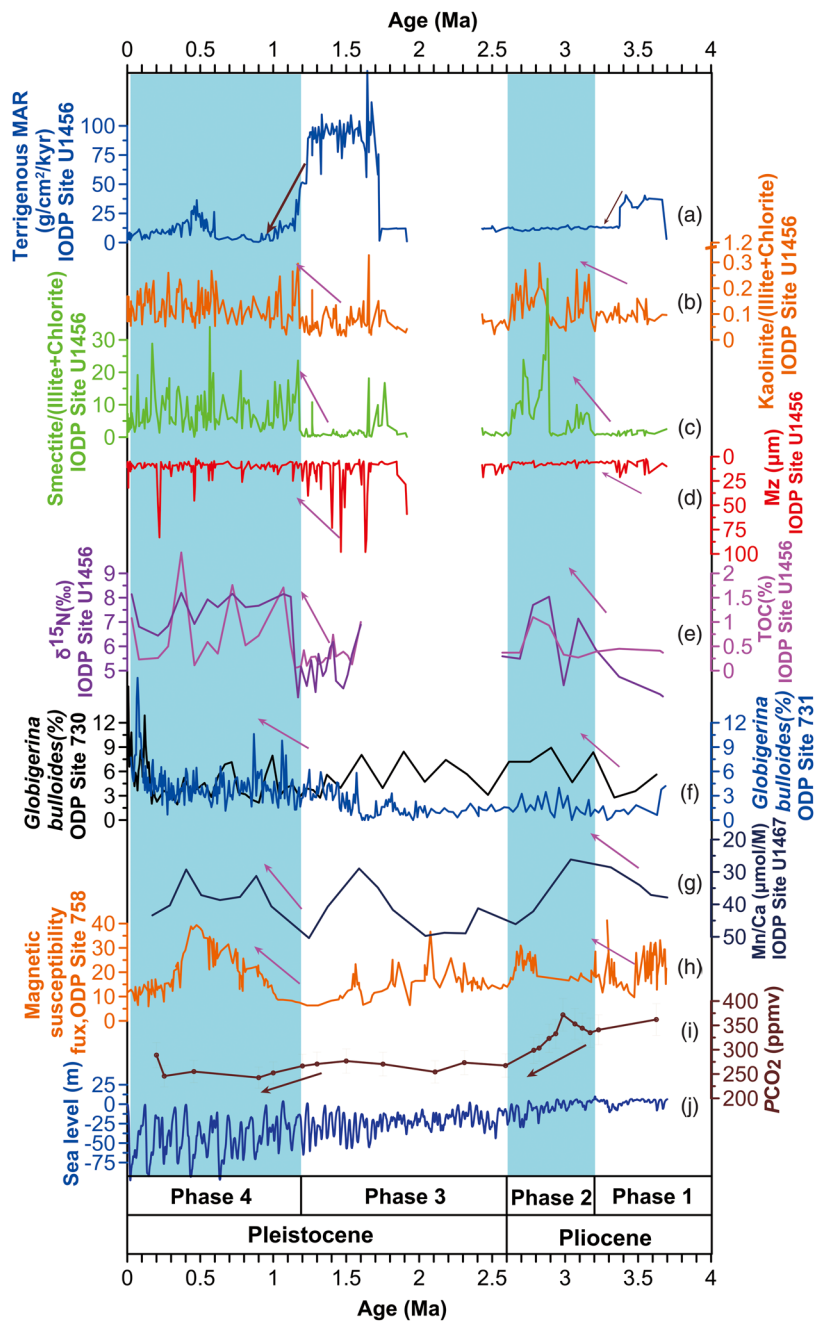


**Fig. 6.** Plots of the mass accumulation rate (MAR) and mean grain size (Mz) of terrigenous materials in addition to the kaolinite/(illite+chlorite) ratio and smectite/(illite+chlorite) ratio from IODP Site U1456 as well as proxy records of the Indian summer monsoon,  $p\text{CO}_2$  and sea level since 3.7 Ma. (a) Terrigenous MAR from IODP Site U1456 (this study), (b) kaolinite/(illite+chlorite) ratio from IODP Site U1456 (this study), (c) smectite/(illite+chlorite) ratio from IODP Site U1456 (this study), (d) mean grain size (Mz) of terrigenous material from IODP Site U1456 (this study), (e) total organic carbon (TOC) content and  $\delta^{15}\text{N}$  value from IODP Site U1456 (Tripathi *et al.* 2017), (f) percentage of *Globigerina bulloides* from ODP Sites 730 (black line, Gupta *et al.* 2015) and 731 (blue line, Gupta *et al.* 2015) in the western Arabian Sea, (g) Mn/Ca record from IODP Site U1467 in the Inner Sea of the Maldives (Betzler *et al.* 2016), (h) magnetic susceptibility record from ODP Site 758 in the southern Bay of Bengal (An *et al.* 2001), (i) atmospheric  $\text{CO}_2$  concentration based on alkenones and boron isotopes (Seki *et al.* 2010) and (j) sea-level change based on eastern Mediterranean  $\delta^{18}\text{O}_p$  values (Rohling *et al.* 2014). The purple arrows represent a strengthening of the monsoon, and the brown arrows indicate a weakening of the monsoon. The blue bands mark the humid periods when many studies, including the present one, indicate strengthened monsoon intensity.

chemical weathering relative to that formed from physical erosion (e.g. Boulay *et al.* 2005; Alizai *et al.* 2012). Because the relative kaolinite content of the sedimentary clay fraction at IODP Site U1456 is very low, the relative kaolinite content should be used as an indicator with caution to determine the chemical weathering intensity therein. In comparison, the smectite/(illite+chlorite) ratio has been successfully used to characterize the chemical weathering intensity in the source areas of clay minerals situated in relatively dry, subtropical regions with extremely low kaolinite contents, such as the Indus River Delta and the Mekong River Delta (Colin *et al.* 2010; Limmer *et al.* 2012). Therefore, the smectite/(illite+chlorite) ratio supplemented with the kaolinite/(illite+chlorite) ratio is primarily used to study the histories of variation in the palaeoclimates and palaeoenvironments of the source areas during various phases.

During phase 1, corresponding to the period from the early Pliocene to the mid-Pliocene, the illite and chlorite contents of the sedimentary clay fraction at IODP Site U1456 were relatively high, whereas the smectite content was relatively low (Fig. 3). The relatively low smectite/(illite+chlorite) ratio (Fig. 6c) and kaolinite/(illite+chlorite) ratio (Fig. 6b) during this phase indicate a relatively weak chemical weathering intensity. A previous study that was based on the TOC and  $\delta^{15}\text{N}$  values (Fig. 6e) of the sediments at IODP Site U1456 showed that the Indian summer monsoon was relatively weak during phase 1 (Tripathi *et al.* 2017). This finding is corroborated by relevant studies on the western Arabian Sea (Gupta *et al.* 2015) (Fig. 6f), the Inner Sea of the Maldives (Betzler *et al.* 2016) (Fig. 6g), and the Bay of Bengal (An *et al.* 2001) (Fig. 6h). Due to a relatively weak Indian summer monsoon and a relatively dry, cold climate (An *et al.* 2001; Cliff *et al.* 2008;

Tripathi *et al.* 2017), the potential source areas were characterized by relatively low monsoon rainfall, resulting in relatively weak and slow chemical weathering coincident with the strong physical erosion of silicates throughout the Himalayan region. In addition, conditions characterized by relatively low rainfall and indistinct seasonal variations were unfavourable for the formation of smectite through the weathering of igneous rocks (Chamley, 1989). Consequently, illite and chlorite were the primary clay mineral components in the weathering and erosion products of the sediments at IODP Site U1456 during phase 1. Due to the weak monsoon rainfall during this phase, the intensity and rate of both the weathering and the erosion of basalts throughout the Deccan Traps were very low (Bluth & Kump, 1994; Dessert *et al.* 2001). Moreover, due to the relatively high sea level at the time (Rohling *et al.* 2014), the palaeo-coastline and the palaeo-estuaries of the western continental margin of India were relatively distant from the study area. Furthermore, the weakening of the Indian summer monsoon reduced the transport capacity of the surface currents in the Arabian Sea, eventually limiting the large-scale transport of the weathering and erosion products (which had already decreased in volume) from the Deccan Traps to the study area (Kessarkar *et al.* 2003; Alizai *et al.* 2012; Limmer *et al.* 2012). Instead, these products may have settled on the continental shelf. This phenomenon was quite common for sediments in the Asian marginal seas controlled by the East and South Asian monsoons (e.g. Rao & Rao, 1995; Kessarkar *et al.* 2003; Li *et al.* 2015). Although the relatively high sea levels at the time could also have caused a retreat of the palaeo-Indus River estuary and the distance between the palaeo-Indus River estuary and the study area was greater than those between the estuaries of rivers crossing the Deccan Traps and the study area, the sedimentary flux of the palaeo-Indus River estuary was significantly greater than that of the rivers crossing the Deccan Traps. In particular, previous research has demonstrated that the uplift of the Himalayan Mountain Range appears to have occurred during the middle Pliocene from 4 to 2 Ma (Rea, 1992). Therefore, the rapid erosion and unroofing of the Himalayan region caused by the uplift of the Himalayan Mountain Range may have been the cause of the high MARs in the study area during phase 1. Thus, some of the detrital material originating from the palaeo-Indus River continued to be transported over long distances by the relatively weak monsoon currents (Shetye *et al.* 1990) before depositing in the study area (Rao & Rao, 1995). Consequently, the palaeo-Indus River was the primary source of detrital clay material at IODP Site U1456 during phase 1, as evidenced by a relatively low smectite/(illite+chlorite) ratio (Fig. 6c), a relatively high smectite crystallinity (Fig. 3i) and a relatively high MAR of terrigenous sediments (Fig. 6a) during this phase. The input of terrigenous clay minerals during phase 1 was significantly affected by the Indian summer monsoon intensity and minimally affected by the sea level. This conclusion is based on the fact that relatively high sea levels should have led to a relative decrease in the sediment input from the Indus River, which would have been relatively distant from the study area, whereas an increase in the sediment input is determined in this work.

Phase 2 corresponds to the warm mid-Pliocene (Haywood *et al.* 2016). During this period, the smectite/(illite+chlorite) ratio (Fig. 6c) and the kaolinite/(illite+chlorite) ratio (Fig. 6b) of the clay minerals in the study area both increased, and the illite crystallinity distinctly decreased (Fig. 3k), suggesting an intensification of chemical weathering during this period. During phase 2, sea level was still relatively high (Rohling *et al.* 2014) (Fig. 6j). The increases

in the TOC and  $\delta^{15}\text{N}$  values of the sediments at IODP Site U1456 (Fig. 6e) indicate an increase in the rainfall associated with Indian summer monsoon (Tripathi *et al.* 2017), which has also been demonstrated in studies on the western Arabian Sea (Gupta *et al.* 2015) (Fig. 6f), the Inner Sea of the Maldives (Betzler *et al.* 2016) (Fig. 6g), and the Bay of Bengal (An *et al.* 2001) (Fig. 6h). The intensity and rate of the weathering and erosion of rocks are both significantly higher in warm, humid environments (Chamley, 1989). Furthermore, basic basalts, which constitute the primary rock type throughout the Deccan Traps, weather far more rapidly than most other rocks in warm, humid environments (Bluth & Kump, 1994; Dessert *et al.* 2001). During phase 2, the temperature was relatively high, and the amount of rainfall increased considerably. Under these conditions, the weathering and erosion rates of the basic basalts in the Deccan Traps would have increased significantly. In addition, the intensification of the Indian summer monsoon also enhanced the transport capacity of the surface currents in the Arabian Sea. As a result, additional weathering and erosion products originating from the basalts of the Deccan Traps entered the eastern Arabian Sea and subsequently affected the mineral composition of the clay fraction in the sediments of the study area. The increased smectite/(illite+chlorite) ratio (Fig. 6c) and the decreased smectite crystallinity (higher smectite crystallinity values in Fig. 3i) during phase 2 both demonstrate that additional weathering and erosion products from the Deccan Traps basalts entered the eastern Arabian Sea. Moreover, the increased temperature and Indian summer monsoon rainfall during phase 2 (Haywood *et al.* 2016) not only increased both the intensity and the rate of silicate weathering and erosion (Wan *et al.* 2012) but also increased the marine biological productivity and rate of TOC burial (Tripathi *et al.* 2017). The accelerated TOC burial is demonstrated by the high TOC content of the sediment (Fig. 6e). The increases in the intensity and rate of chemical weathering of rocks and in the rate of TOC burial resulted in the consumption of large amounts of  $\text{CO}_2$ , leading to a decrease in the atmospheric  $\text{CO}_2$  concentration (Seki *et al.* 2010) (Fig. 6i), which eventually resulted in the development of Northern Hemisphere ice sheets and global climate cooling at  $\sim 2.7$  Ma (Berger & Loutre, 1991; Molnar *et al.* 2010; Rohling *et al.* 2014). Therefore, the change in the intensity of the Indian summer monsoon was the primary factor that caused IODP Site U1456 to receive more detrital clay material from the Deccan Traps during 3.2–2.6 Ma.

Phase 3 corresponds to the early Pleistocene. Compared with phase 2, the relative percentage contents increased significantly for illite and chlorite but decreased significantly for smectite (Fig. 3d, e, g). The significantly lower smectite/(illite+chlorite) ratio (Fig. 6c), kaolinite/(illite+chlorite) ratio (Fig. 6b), and illite crystallinity values during phase 3 relative to phase 2 suggest relatively weak chemical weathering intensity during phase 3. The decreased  $\delta^{15}\text{N}$  and TOC values of the sediments at IODP Site U1456 (Fig. 6e) indicate a weaker Indian summer monsoon and a relatively dry, cold climate during this phase (Tripathi *et al.* 2017), which are consistent with research results from adjacent marine areas (Fig. 6f, g, h) (An *et al.* 2001; Sun *et al.* 2006; Huang *et al.* 2007; Zhang *et al.* 2009; Gupta *et al.* 2015; Betzler *et al.* 2016). The start of phase 3 coincided with the initial development of Northern Hemisphere ice sheets (Berger & Loutre, 1991; Maslin *et al.* 2001). This development of ice sheets resulted in a rapid decrease in the global sea level at  $\sim 2.6$  Ma (Rohling *et al.* 2014), causing the regression of the palaeo-coastline and exposing large areas of the continental shelf. This process consequently reduced the distances between the palaeo-estuaries of the rivers



on the Indian subcontinent and the study area. As a result, detrital materials originating from the Deccan Traps should theoretically have been more easily transported to IODP Site U1456. However, with the weakening of the Indian summer monsoon and the corresponding reduction in monsoon rainfall (An *et al.* 2001; Sun *et al.* 2006; Huang *et al.* 2007; Gupta *et al.* 2015; Betzler *et al.* 2016), the chemical weathering intensity of the Deccan Traps basalts decreased significantly, resulting in significant decreases in the runoff and suspended sediment contents of small regional rivers on the Deccan Traps (e.g. the Narmada and Tapti Rivers) entering the eastern Arabian Sea. In addition, the weakening of the Indian summer monsoon weakened the transport capacity of the surface currents in the Arabian Sea, hindering the transport of weathering and erosion products (the volume of which had also decreased) from the Deccan Traps to the study area. However, the sedimentary flux of the palaeo-Indus River estuary was significantly greater than those of the rivers crossing the Deccan Traps. Thus, some of the detrital material originating from the palaeo-Indus River continued to be transported over long distances by the relatively weak monsoon currents before settling in the study area. As a result, the Indus River remained the primary source of terrigenous material in the study area (Fig. 6b, c). Therefore, the weakening of the Indian monsoon was the main reason why the terrigenous materials in the sediments from the eastern Arabian Sea primarily originated from the Indus River during 2.6–1.2 Ma. The significant decrease in the smectite/(illite+chlorite) ratio during phase 3 was due to at least two reasons. First, the relatively low temperature and low rainfall significantly reduced the intensity and rate of basalt weathering in the Deccan Traps, thereby considerably reducing the transport of smectite-rich clay into the eastern Arabian Sea. Second, during this phase, the intensity and rate of silicate chemical weathering in the Himalayan region decreased, whereas the physical weathering of silicates intensified, resulting in increases in the illite and chlorite proportions in the weathering and erosional clay products.

Notably, during 1.7–1.2 Ma, the MAR of the terrigenous sediment at IODP Site U1456 (Fig. 6a) significantly increased, as did the detrital sediment particle size (Fig. 6d). Furthermore, the smectite crystallinity improved (lower smectite crystallinity values in Fig. 3i). These changes cannot be interpreted using the sea-level fluctuations and monsoon rainfall intensity alone. Previous research has demonstrated that the Tibetan Plateau experienced intense tectonic compressive deformation during 1.7–1.3 Ma (Wu & An, 1996), resulting in rapid erosion and unroofing of the Himalayan region. This event is consistent with the rapid multi-fold increase in the MAR during 1.7–1.2 Ma observed in our data. Therefore, the rapid erosion and unroofing of the Himalayan region caused by the tectonic compressive deformation of the Tibetan Plateau may have been the cause of the high MARs in the study area during 1.7–1.2 Ma (Wu & An, 1996; Meng *et al.* 2011). This rapid erosion and unroofing produced large amounts of detrital material that entered the eastern Arabian Sea, resulting in an increase in the illite content of the clay fraction (Fig. 3e). In addition, Clift & Blusztajn (2005) argued that the river systems throughout the western Himalaya started to experience a major reorganization at ~2 Ma and that this reorganization was the primary cause of both the relatively low MARs in the Pliocene and the significantly increased MARs in the Pleistocene in the Arabian Sea. This conclusion is consistent with our results (Fig. 6a). A river flowing through the current Punjab State of India in the western Himalayan Mountain Range that was once a branch of the Ganges River changed its course and began to flow into the Indus River during the Pliocene (Clift & Blusztajn, 2005). This reorganization may have contributed to the significant increase in

the MAR of terrigenous materials at IODP Site U1456 during this phase.

Phase 4 is characterized by a relatively low detrital sediment MAR (Fig. 6a), a relatively high kaolinite/(illite+chlorite) ratio (Fig. 6b), a relatively high smectite/(illite+chlorite) ratio (Fig. 6c), a relatively small sediment particle size (Fig. 6d) and a relatively low smectite crystallinity (higher smectite crystallinity values in Fig. 3i), suggesting a relatively strong chemical weathering intensity and an increased input of weathering and erosion products from the Deccan Traps basalts to the sedimentary deposition in the eastern Arabian Sea. Phase 4 is also characterized by a relatively low sea level (Rohling *et al.* 2014) (Fig. 6j) but high TOC and  $\delta^{15}\text{N}$  sediment values at IODP Site U1456 (Fig. 6e), indicating a re-intensification of the Indian summer monsoon and a relative increase in monsoon rainfall over South Asia (Tripathi *et al.* 2017). The same conclusion regarding the monsoon intensity during this phase was reached in related research on the western Arabian Sea (Gupta *et al.* 2015) (Fig. 6f), the Inner Sea of the Maldives (Betzler *et al.* 2016) (Fig. 6g), and the Bay of Bengal (An *et al.* 2001) (Fig. 6h). The strengthened Indian summer monsoon and the increased monsoon rainfall considerably accelerated the weathering and erosion of the basalts in the Deccan Traps (Bluth & Kump, 1994; Dessert *et al.* 2001). Furthermore, the relatively low sea level during this phase also shortened the distances between the palaeo-estuaries on the Deccan Traps and the eastern Arabian Sea, and the stronger Indian summer monsoon increased the transport capacity of the surface currents. As a result, additional detrital clay materials originating from the Deccan Traps were deposited in the study area. Therefore, the intensification of the Indian summer monsoon was the primary factor causing the relative changes in the content of terrigenous material delivered to the eastern Arabian Sea from the Deccan Traps and the Indus River. Moreover, the decline in the sea level may also have been a factor causing the aforementioned changes. Notably, the experimental data obtained in this work show relatively low illite crystallinity values during this phase, which is inconsistent with the chemical weathering intensification caused by the strengthened Indian summer monsoon in the study area. This phenomenon may be attributable to the fact that low-crystallinity illite (higher illite crystallinity values) forms in warm, high-rainfall climates, whereas continuous cooling in the Northern Hemisphere beginning at 1.2 Ma (Berger & Loutre, 1991) resulted primarily in the formation of high-crystallinity illite (lower illite crystallinity values) in the Himalayan region with high elevations. In addition, during phase 4, the detrital sediment MAR significantly decreased as the Indian summer monsoon intensified and the rainfall increased (Fig. 6a). One possible cause is the cessation of rapid erosion and unroofing of the Himalayan region caused by the compressive deformation of the Tibetan Plateau since 1.2 Ma (Wu & An, 1996; Meng *et al.* 2011); consequently, the rate of erosion in the Himalayan region decreased considerably. Another possible cause is the continuous cooling of the Northern Hemisphere since 1.2 Ma (Berger & Loutre, 1991) that has resulted in an increase in the areal coverage of ice sheets over the relatively high-elevation Greater Himalayan region; this process consequently decreased the area of exposed rocks in the Himalayan region and eventually decreased the total seaward flux of terrigenous materials formed through the weathering and erosion of rocks (Wu & An, 1996; Tripathy *et al.* 2014).

In summary, the input of terrigenous clay material to IODP Site U1456 was primarily controlled by the monsoon climates in the potential source areas during each period. Starting at 3.7 Ma, terrigenous clay sediments in the eastern Arabian Sea were mainly

derived from the Indus River and were periodically supplied by the weathering and erosion of the basalts throughout the Deccan Traps. Subsequently, with the weakening of the South Asian monsoon intensity, the chemical weathering of the source area diminished, relatively large amounts of illite and chlorite formed, and the clay fraction of the terrigenous sediment in the study area was primarily derived from the Indus River. Then, relatively large amounts of smectite formed and additional detrital clay materials originating from the Deccan Traps entered the eastern Arabian Sea when the chemical weathering in the source areas intensified with the strengthening of the Indian summer monsoon and an increase in rainfall. Therefore, the Indian summer monsoon intensity has been the primary factor controlling the relative inputs of weathering and erosion products from the Deccan Traps and the Indus River into the eastern Arabian Sea. In addition, the transport of terrigenous material into the eastern Arabian Sea may have been affected by several secondary factors, such as the tectonic compressive deformation of the Tibetan Plateau, the sea level, and the reorganization of the Indus River system. Moreover, the proportion of clay minerals formed from chemical weathering relative to those formed from physical weathering (characterized by the smectite/(illite+chlorite) ratio) has been significantly coupled to the Indian summer monsoon intensity since the Pliocene (Fig. 6). The intensification of the Indian summer monsoon caused the smectite/(illite+chlorite) ratio to increase, whereas the weakening of the Indian summer monsoon caused the smectite/(illite+chlorite) ratio to decrease.


## 5. Conclusions

The clay minerals in the sediments from 3.7 Ma to the present day at IODP Site U1456 mainly consist of smectite, illite, chlorite and kaolinite. Smectite (0–90%, average 44%) and illite (3–90%, average 44%) are the primary components, while chlorite (1–26%, average 7%) and kaolinite (0–19%, average 5%) are the secondary components. Based on the characteristics of and variations in the relative contents of the four clay components (i.e. smectite, illite, chlorite and kaolinite), the sedimentary record is divided into the following four phases: phase 1 (early Pliocene to mid-Pliocene, 3.7–3.2 Ma), phase 2 (mid-Pliocene, 3.2–2.6 Ma), phase 3 (late Pliocene to early Pleistocene, 2.6–1.2 Ma) and phase 4 (early Pleistocene to the present, 1.2–0 Ma). During phases 1 and 3, the illite contents were relatively high (with averages of 60% and 63%, respectively), whereas the smectite contents during phases 2 and 4 were relatively high (with averages of 56% and 59%, respectively).

Provenance analysis results show that the clay-sized siliciclastic sediments at IODP Site U1456 were mainly derived from the Indus River during 3.7–3.2 Ma and 2.6–1.2 Ma. Furthermore, the contributions of siliciclastic sediments from the Deccan Traps to this site increased considerably during 3.2–2.6 Ma and 1.2–0 Ma.

Since the Pliocene, the input of the clay fraction of terrigenous sediment in the eastern Arabian Sea has been primarily controlled by the Indian summer monsoon intensity on a tectonic scale. In other words, changes in the intensity of the Indian summer monsoon were mainly responsible for the changes in the composition of the terrigenous sediment at IODP Site U1456 at 3.2 Ma, 2.6 Ma and 1.2 Ma. When the Indian summer monsoon weakened, the intensity and rate of chemical weathering in the source areas (particularly the chemical weathering of basalts in the Deccan Traps) decreased. Consequently, the terrigenous sediment (characterized by high illite and chlorite contents) was mainly derived from the Indus River, which is rich in illite and chlorite. When the Indian summer

monsoon rainfall increased, the intensity and rate of weathering in the source areas (particularly the weathering of basalts in the Deccan Traps) increased. Consequently, the terrigenous sediment input (characterized by a high smectite content) from the Deccan Traps increased significantly. On a tectonic timescale, the relationship between the proportion of clay minerals formed by chemical weathering and that formed by physical weathering (characterized by the smectite/(illite+chlorite) ratio) and the Indian summer monsoon intensity has exhibited significant coupling since the Pliocene. As the Indian summer monsoon intensified, the smectite/(illite+chlorite) ratio increased, and as the Indian summer monsoon weakened, the smectite/(illite+chlorite) ratio decreased.

**Author ORCIDs.**  Mingjiang Cai 0000-0003-4362-8810, Boo-Keun Kim 0000-0002-0229-7990, Denise K. Kulhanek 0000-0002-2156-6383

**Acknowledgements.** This research used samples provided by the International Ocean Discovery Program (IODP). The authors acknowledge Jie Huang, Jin Zhang and Hongli Wang for their great assistance with the sample analyses. Funding for this research was provided by the National Natural Science Foundation of China (41676038 and 41876034), the Scientific and Technological Innovation Project Financially Supported by Qingdao National Laboratory for Marine Science and Technology (2016ASKJ13), the National Special Project for Global Change and Air–Sea Interaction (GASI-GEOGE-02, GASI-GEOGE-04 and GASI-GEOGE-06-02), the NSFC–Shandong Joint Fund for Marine Science Research Centers (U1606401), the strategic Priority Research Program of the Chinese Academy of Sciences (XDA11030104), the National Research Foundation of Korea (2016K2A9A2A08003704 and 2016R1A2B4008256), the Korea Institute of Ocean Science & Technology (PE99606), and the Shandong Provincial Natural Science Foundation, China (ZR2016DM12). P.D.C.’s involvement was by means of the Charles T. McCord Jr Chair in Petroleum Geology.

## References

- Alizai, A, Hillier, S, Clift, PD, Giosan, L, Hurst, A, Vanlaningham, S and Macklin, M (2012) Clay mineral variations in Holocene terrestrial sediments from the Indus basin. *Quaternary Research* 77, 368–81.
- Allen, MB and Armstrong, HA (2012) Reconciling the Intertropical Convergence Zone, Himalayan/Tibetan tectonics, and the onset of the Asian monsoon system. *Journal of Asian Earth Sciences* 44, 36–47.
- An, Z, Kutzbach, JE, Prell, WL and Porter, SC (2001) Evolution of Asian monsoons and phased uplift of the Himalaya–Tibetan plateau since Late Miocene times. *Nature* 411, 62–6.
- Armstrong, HA and Allen, MB (2011) Shifts in the intertropical convergence zone, Himalayan exhumation, and late Cenozoic climate. *Geology* 39, 11–14.
- Avinash, K, Kurian, PJ, Warriar, AK, Shankar, R, Vineesh, TC and Ravindra, R (2016) Sedimentary sources and processes in the eastern Arabian Sea: insights from environmental magnetism, geochemistry and clay mineralogy. *Geoscience Frontiers* 7, 253–64.
- Bayon, G, German, CR, Boella, RM, Milton, JA, Taylor, RN and Nesbitt, RW (2002) An improved method for extracting marine sediment fractions and its application to Sr and Nd isotopic analysis. *Chemical Geology* 187, 179–99.
- Beaumont, C, Jamieson, RA, Nguyen, MH and Lee, B (2001) Himalayan tectonics explained by extrusion of a low-viscosity crustal channel coupled to focused surface denudation. *Nature* 414, 738–42.
- Berger, A and Loutre, MF (1991) Insolation values for the climate of the last 10 million years. *Quaternary Science Reviews* 10, 297–317.
- Betzler, C, Eberli, GP, Kroon, D, Wright, JD, Swart, PK, Nath, BN, Alvarez-Zarikian, C, Alonso-García, M, Bialik, OM, Blättler, CL, Guo, JA, Haffen, S, Horoza, S, Inoue, M, Jovane, L, Lanci, L, Laya, JC, Mee, ALH, Lüdmann, T, Nakakuni, M, Niino, K, Petruny, LM, Pratiw, SD, Reijmer, JJG, Reolid, J, Slagle, AL, Sloss, CR, Su, X, Yao, Z and Young, JR (2016) The abrupt onset of the modern South Asian Monsoon winds. *Scientific Reports* 6. doi: 10.1038/srep29838.
- Biscaye, PE (1965) Mineralogy and sedimentation of recent deep-sea clay in the Atlantic Ocean and adjacent seas and oceans. *Geological Society of America Bulletin* 76, 803–32.

- Bluth, GJ and Kump, LR (1994)** Lithologic and climatologic controls of river chemistry. *Geochimica et Cosmochimica Acta* **58**, 2341–59.
- Boulay, S, Colin, C, Trentesaux, A, Frank, N and Liu, Z (2005)** Sediment sources and East Asian monsoon intensity over the last 450 ky. Mineralogical and geochemical investigations on South China Sea sediments. *Palaeogeography, Palaeoclimatology, Palaeoecology* **228**, 260–77.
- Boulay, S, Colin, C, Trentesaux, A, Pluquet, F, Bertaux, J, Blamart, D, Buchring, C and Wang, P (2003)** Mineralogy and sedimentology of Pleistocene sediment in the South China Sea (ODP Site 1144). *Proceedings of the Ocean Drilling Program, Scientific Results* **184**, 1–21.
- Bouquillon, A, Chamley, H and Frohlich, F (1989)** Sédimentation argileuse au cénozoïque supérieur dans l'Océan Indien nord-oriental. *Oceanologica Acta* **12**, 133–47.
- Cabarcos, E, Flores, JA, Singh, AD and Sierro, FJ (2014)** Monsoonal dynamics and evolution of the primary productivity in the eastern Arabian Sea over the past 30 ka. *Palaeogeography, Palaeoclimatology, Palaeoecology* **411**, 249–56.
- Campbell, IB and Claridge, GGC (1982)** The influence of moisture on the development of soils of the cold deserts of Antarctica. *Geoderma* **28**, 221–38.
- Chamley, H (1989)** Clay Sedimentology. Berlin: Springer-Verlag, 626 pp. .
- Clift, PD and Blusztajn, J (2005)** Reorganization of the western Himalayan river system after five million years ago. *Nature* **438**, 1001–3.
- Clift, PD, Hodges, KV, Heslop, D, Hannigan, R, Van Long, H and Calves, G (2008)** Correlation of Himalayan exhumation rates and Asian monsoon intensity. *Nature Geoscience* **1**, 875–80.
- Clift, PD, Shimizu, N, Layne, GD, Blusztajn, JS, Gaedicke, C, Schluter, HU, Clark, MK and Amjad, S (2001)** Development of the Indus Fan and its significance for the erosional history of the Western Himalaya and Karakoram. *Geological Society of America Bulletin* **113**, 1039–51.
- Clift, PD, Wan, S and Blusztajn, J (2014)** Reconstructing chemical weathering, physical erosion and monsoon intensity since 25 Ma in the northern South China Sea: a review of competing proxies. *Earth-Science Reviews* **130**, 86–102.
- Colin, C, Siani, G, Sicre, MA and Liu, Z (2010)** Impact of the East Asian monsoon rainfall changes on the erosion of the Mekong River basin over the past 25,000 yr. *Marine Geology* **271**, 84–92.
- Curray, JR (1994)** Sediment volume and mass beneath the Bay of Bengal. *Earth and Planetary Science Letters* **125**, 371–83.
- Debrabant, P, Krisek, L, Bouquillon, A and Chamley, H (1991)** Clay mineralogy of Neogene sediments of the western Arabian Sea: mineral abundances and paleoenvironmental implications. *Proceedings of the Ocean Drilling Program, Scientific Results* **117**, 183–6.
- Derry, LA and France-Lanord, C (1996)** Neogene Himalayan weathering history and river  $^{87}\text{Sr}/^{86}\text{Sr}$ : impact on the marine Sr record. *Earth and Planetary Science Letters* **142**, 59–74.
- Dessert, C, Durpe, B, François, LM, Schott, J, Gaillardet, J, Chakrapani, G and Bajpai, S (2001)** Erosion of Deccan Traps determined by river geochemistry: impact on the global climate and the  $^{87}\text{Sr}/^{86}\text{Sr}$  ratio of seawater. *Earth and Planetary Science Letters* **188**, 459–74.
- Fleitmann, D, Burns, SJ, Mudelsee, M, Neff, U, Kramers, J, Mangini, A and Matter, A (2003)** Holocene forcing of the Indian monsoon recorded in a stalagmite from southern Oman. *Science* **300**, 1737–9.
- France-Lanord, C and Derry, LA (1997)** Organic carbon burial forcing of the carbon cycle from Himalayan erosion. *Nature* **390**, 65–7.
- Garzanti, E, Vezzoli, G, Ando, S, Paparella, P and Clift, PD (2005)** Petrology of Indus River sands: a key to interpret erosion history of the Western Himalayan Syntaxis. *Earth and Planetary Science Letters* **229**, 287–302.
- Gingele, FX, Müller, PM and Schneider, RR (1998)** Orbital forcing of freshwater input in the Zaire Fan area: clay mineral evidence from the last 200 kyr. *Palaeogeography, Palaeoclimatology, Palaeoecology* **138**, 17–26.
- Giosan, L, Constantinescu, S, Clift, PD, Tabrez, AR, Danish, M and Inam, A (2006)** Recent morphodynamics of the Indus delta shore and shelf. *Continental Shelf Research* **26**, 1668–84.
- Gupta, AK, Yuvaraja, A, Prakasam, M, Clemens, SC and Velu, A (2015)** Evolution of the South Asian monsoon wind system since the late Middle Miocene. *Palaeogeography, Palaeoclimatology, Palaeoecology* **438**, 160–7.
- Gutjahr, M, Frank, M, Stirling, CH, Klemm, V, Van de Flierdt, T and Halliday, AN (2007)** Reliable extraction of a deepwater trace metal isotope signal from Fe-Mn oxyhydroxide coatings of marine sediments. *Chemical Geology* **242**, 351–70.
- Haywood, AM, Dowsett, HJ and Dolan, AM (2016)** Integrating geological archives and climate models for the mid-Pliocene warm period. *Nature Communications* **7**, 1–14.
- Hu, D, Böning, P, Köhler, CM, Hillier, S, Pressling, N, Wan, S, Brumsack, HJ and Clift, PD (2012)** Deep sea records of the continental weathering and erosion response to East Asian monsoon intensification since 14ka in the South China Sea. *Chemical Geology* **326**, 1–18.
- Huang, Y, Clemens, SC, Liu, W, Wang, Y and Prell, WL (2007)** Large-scale hydrological change drove the late Miocene C4 plant expansion in the Himalayan foreland and Arabian Peninsula. *Geology* **35**, 531–4.
- Ivanova, E, Schiebel, R, Singh, AD, Schmiedl, G, Niebler, HS and Hemleben, C (2003)** Primary production in the Arabian Sea during the last 135 000 years. *Palaeogeography, Palaeoclimatology, Palaeoecology* **197**, 61–82.
- Jeong, GY, Yoon, HI and Lee, SY (2004)** Chemistry and microstructures of clay particles in smectite-rich shelf sediments, South Shetland Islands, Antarctica. *Marine Geology* **209**, 19–30.
- Kessarkar, PM, Rao, VP, Ahmad, SM and Babu, GA (2003)** Clay minerals and Sr-Nd isotopes of the sediments along the western margin of India and their implication for sediment provenance. *Marine Geology* **202**, 55–69.
- Kolla, V and Coumes, F (1987)** Morphology, internal structure, seismic stratigraphy, and sedimentation of Indus Fan. *AAPG Bulletin* **71**, 650–77.
- Kolla, V, Kosteckí, JA, Robinson, F, Biscaye, PE and Ray, PK (1981)** Distributions and origins of clay minerals and quartz in surface sediments of the Arabian Sea. *Journal of Sedimentary Research* **51**, 563–9.
- Kuwahara, Y, Masudome, Y, Paudel, MR, Fujii, R, Hayashi, T, Mampuku, M and Sakai, H (2010)** Controlling weathering and erosion intensity on the southern slope of the Central Himalaya by the Indian summer monsoon during the last glacial. *Global and Planetary Change* **71**, 73–84.
- Li, T, Xu, Z, Lim, D, Chang, F, Wan, S, Jung, H and Choi, J (2015)** Sr-Nd isotopic constraints on detrital sediment provenance and paleoenvironmental change in the northern Okinawa Trough during the late Quaternary. *Palaeogeography, Palaeoclimatology, Palaeoecology* **430**, 74–84.
- Limmer, DR, Köhler, CM, Hillier, S, Moreton, SG, Tabrez, AR and Clift, PD (2012)** Chemical weathering and provenance evolution of Holocene-recent sediments from the Western Indus Shelf, Northern Arabian Sea inferred from physical and mineralogical properties. *Marine Geology* **326**, 101–15.
- Liu, X, Dong, H, Yang, X, Herzsuh, U, Zhang, E, Stuut, JBW and Wang, Y (2009)** Late Holocene forcing of the Asian winter and summer monsoon as evidenced by proxy records from the northern Qinghai-Tibetan Plateau. *Earth and Planetary Science Letters* **280**, 276–84.
- Liu, Z, Colin, C, Trentesaux, A, Blamart, D, Bassinot, F, Siani, G and Sicre, MA (2004)** Erosional history of the eastern Tibetan Plateau since 190 kyr ago: clay mineralogical and geochemical investigations from the southwestern South China Sea. *Marine Geology* **209**, 1–18.
- Liu, Z, Trentesaux, A, Clemens, SC, Colin, C, Wang, P, Huang, B and Boulay, S (2003)** Clay mineral assemblages in the northern South China Sea: implications for East Asian monsoon evolution over the past 2 million years. *Marine Geology* **201**, 133–46.
- Liu, Z, Zhao, Y, Colin, C, Statterger, K, Wiesner, MG, Huh, CA, Zhang, YW, Li, XJ, Sompongchaiyakul, P, You, CF, Huang, CY, Liu, JT, Siringan, FP, Le, KP, Sathiamurthy, E, Hantoro, WS, Liu, JG, Tuo, S and Li, YL (2016)** Source-to-sink transport processes of fluvial sediments in the South China Sea. *Earth-Science Reviews* **153**, 238–73.
- Maslin, M, Seidov, D and Lowe, J (2001)** Synthesis of the nature and causes of rapid climate transitions during the Quaternary. *The Oceans and Rapid Climate Change* **126**, 9–52.
- Meng, X, Xia, P, Zheng, J and Wang, X (2011)** Evolution of the East Asian monsoon and its response to uplift of the Tibetan Plateau since 1.8 Ma recorded by major elements in sediments of the South China Sea. *Chinese Science Bulletin* **56**, 547–51.
- Milliman, JD and Farnsworth, KL (2013)** *River Discharge to the Coastal Ocean: A Global Synthesis*. Cambridge: Cambridge University Press.
- Molnar, P, Boos, WR and Battisti, DS (2010)** Orographic controls on climate and paleoclimate of Asia: thermal and mechanical roles for the Tibetan Plateau. *Annual Review of Earth and Planetary Sciences* **38**, 77–102.
- Molnar, P, England, P and Martinod, J (1993)** Mantle dynamics, uplift of the Tibetan Plateau, and the Indian monsoon. *Reviews of Geophysics* **31**, 357–96.

- Overpeck, J, Anderson, D, Trumbore, S and Prell, W (1996) The southwest Indian Monsoon over the last 18 000 years. *Climate Dynamics* **12**, 213–25.
- Pandey, DK, Clift, PD and Kulhanek, DK (2016) Site 1456. *Proceedings of the International Ocean Discovery Program* **355**, 1–61.
- Phillips, SC, Johnson, JE, Underwood, MB, Guo, J, Giosan, L and Rose, K (2014) Long-timescale variation in bulk and clay mineral composition of Indian continental margin sediments in the Bay of Bengal, Arabian Sea, and Andaman Sea. *Marine and Petroleum Geology* **58**, 117–38.
- Prell, WL and Kutzbach, JE (1992) Sensitivity of the Indian monsoon to forcing parameters and implications for its evolution. *Nature* **360**, 647–52.
- Prins, MA, Postma, G, Cleveringa, J, Cramp, A and Kenyon, NH (2000) Controls on terrigenous sediment supply to the Arabian Sea during the late Quaternary: the Indus Fan. *Marine Geology* **169**, 327–49.
- Rao, VP and Rao, BR (1995) Provenance and distribution of clay minerals in the sediments of the western continental shelf and slope of India. *Continental Shelf Research* **15**, 1757–71.
- Raymo, ME, Ruddiman, WF and Froelich, PN (1988) Influence of late Cenozoic mountain building on ocean geochemical cycles. *Geology* **16**, 649–53.
- Rea, DK (1992) Delivery of Himalayan sediment to the northern Indian Ocean and its relation to global climate, sea level, uplift, and seawater strontium. *Synthesis of Results from Scientific Drilling in the Indian Ocean* **70**, 387–402.
- Rea, DK, Snoeckx, H and Joseph, LH (1998) Late Cenozoic eolian deposition in the North Pacific: Asian drying, Tibetan uplift, and cooling of the northern hemisphere. *Paleoceanography* **13**, 215–24.
- Rohling, EJ, Foster, GL, Grant, KM, Marino, G, Roberts, AP, Tamisiea, ME and Williams, F (2014) Sea-level and deep-sea-temperature variability over the past 5.3 million years. *Nature* **508**, 477–82.
- Seki, O, Foster, GL, Schmidt, DN, Mackensen, A, Kawamura, K and Pancost, RD (2010) Alkenone and boron-based Pliocene pCO<sub>2</sub> records. *Earth and Planetary Science Letters* **292**, 201–11.
- Shetye, SR, Gouveia, AD, Shenoi, SSC, Sundar, D, Michael, GS, Almeida, AM and Santanam, K (1990) Hydrography and circulation off the west coast of India during the southwest monsoon 1987. *Journal of Marine Research* **48**, 359–78.
- Singh, AD, Jung, SJ, Darling, K, Ganeshram, R, Ivanochko, T and Kroon, D (2011) Productivity collapses in the Arabian Sea during glacial cold phases. *Paleoceanography and Paleoclimatology* **26**, PA3210. doi: [10.1029/2009PA001923](https://doi.org/10.1029/2009PA001923).
- Singh, AD, Kroon, D and Ganeshram, RS (2006) Millennial scale variations in productivity and OMZ intensity in the eastern Arabian Sea. *Journal of the Geological Society of India* **68**, 369–77.
- Sirocko, F and Lange, H (1991) Clay-mineral accumulation rates in the Arabian Sea during the late Quaternary. *Marine Geology* **97**, 105–19.
- Sun, D, Shaw, J, An, Z, Cheng, M and Yue, L (1998) Magnetostratigraphy and paleoclimatic interpretation of a continuous 7.2 Ma Late Cenozoic eolian sediment from the Chinese Loess Plateau. *Geophysical Research Letters* **25**, 85–8.
- Sun, Y, An, Z, Clemens, SC, Bloemendal, J and Vandenberghe, J (2010) Seven million years of wind and precipitation variability on the Chinese Loess Plateau. *Earth and Planetary Science Letters* **297**, 525–35.
- Sun, Y, Lu, H and An, Z (2006) Grain size of loess, palaeosol and Red Clay deposits on the Chinese Loess Plateau: significance for understanding pedogenic alteration and palaeomonsoon evolution. *Palaeogeography, Palaeoclimatology, Palaeoecology* **241**, 129–38.
- Tada, R, Murray, RW and Alvarez Zarikian, CA (2013) Asian monsoon: onset and evolution of millennial-scale variability of Asian monsoon and its possible relation with Himalaya and Tibetan Plateau uplift. *Integrated Ocean Drilling Program Preliminary Reports*, **346**. College Station, Texas.
- Tada, R, Zheng, H and Clift, PD (2016) Evolution and variability of the Asian monsoon and its potential linkage with uplift of the Himalaya and Tibetan Plateau. *Progress in Earth and Planetary Science* **3**, 1–26.
- Thamban, M, Rao, VP and Schneider, RR (2002) Reconstruction of late Quaternary monsoon oscillations based on clay mineral proxies using sediment cores from the western margin of India. *Marine Geology* **186**, 527–39.
- Thiede, RC, Bookhagen, B, Arrowsmith, JR, Sobel, ER and Strecker, MR (2004) Climatic control on rapid exhumation along the Southern Himalayan Front. *Earth and Planetary Science Letters* **222**, 791–806.
- Thiry, M (2000) Palaeoclimatic interpretation of clay minerals in marine deposits: an outlook from the continental origin. *Earth-Science Reviews* **49**, 201–21.
- Tripathi, S, Tiwari, M, Lee, J, Khim, BK and IODP Expedition 355 Scientists (2017) First evidence of denitrification vis-à-vis monsoon in the Arabian Sea since Late Miocene. *Scientific Reports* **7**, 43–56.
- Tripathy, GR, Singh, SK and Ramaswamy, V (2014) Major and trace element geochemistry of Bay of Bengal sediments: implications to provenances and their controlling factors. *Palaeogeography, Palaeoclimatology, Palaeoecology* **397**, 20–30.
- Wan, S, Clift, PD, Li, A, Yu, Z, Li, T and Hu, D (2012) Tectonic and climatic controls on long-term silicate weathering in Asia since 5 Ma. *Geophysical Research Letters* **39**, 151–5.
- Wan, S, Clift, PD, Zhao, D, Hovius, N, Munhoven, G, France-Lanord, C, Wang, Y, Xiong, Z, Huang, J, Yu, Z, Zhang, J, Ma, W, Zhang, G, Li, A and Li, T (2017) Enhanced silicate weathering of tropical shelf sediments exposed during glacial lowstands: a sink for atmospheric CO<sub>2</sub>. *Geochimica et Cosmochimica Acta* **200**, 123–44.
- Wan, S, Li, A, Clift, PD and Stuut, JBW (2007) Development of the East Asian monsoon: mineralogical and sedimentologic records in the northern South China Sea since 20 Ma. *Palaeogeography, Palaeoclimatology, Palaeoecology* **254**, 561–82.
- Wu, X and An, Z (1996) Loess-paleosol sequence on Loess Plateau and uplift of the Qinghai-Xizang Plateau. *Science in China Series D – Earth Sciences* **39**, 121–33.
- Xu, Z, Li, T, Clift, PD, Lim, D, Wan, S, Chen, H, Tang, Z, Jiang, F and Xiong, Z (2015) Quantitative estimates of Asian dust input to the western Philippine Sea in the mid-late Quaternary and its potential significance for paleoenvironment. *Geochemistry, Geophysics, Geosystems* **16**, 3182–96.
- Xu, Z, Li, T, Clift, PD, Wan, S, Cai, M and Chen, H (2016) Comment on “Sr-Nd isotope composition and clay mineral assemblages in Eolian dust from the central Philippine Sea over the last 600 kyr: implications for the transport mechanism of Asian dust” by Seo et al. *Journal of Geophysical Research: Atmospheres* **121**, 14137–41.
- Yu, Z, Wan, S, Colin, C, Yan, H, Bonneau, L, Liu, ZF, Song, LN, Sun, HJ, Xu, ZK, Jiang, XJ, Li, AC and Li, TG (2016) Co-evolution of monsoonal precipitation in East Asia and the tropical Pacific ENSO system since 2.36 Ma: new insights from high-resolution clay mineral records in the West Philippine Sea. *Earth and Planetary Science Letters* **446**, 45–55.
- Zhang, YG, Ji, J, Balsam, W, Liu, L and Chen, J (2009) Mid-Pliocene Asian monsoon intensification and the onset of Northern Hemisphere glaciation. *Geology* **37**, 599–602.